ELSEVIER

Journal of Organometallic Chemistry 628 (2001) 222–232

Journal of Organometallic Chemistry

www.elsevier.nl/locate/jorganchem

Reaction mechanism of the reductive elimination in the catalytic carbonylation of methanol. A density functional study

Tapani Kinnunen, Kari Laasonen *

Department of Chemistry, University of Oulu, P.O. Box 3000, FIN-90014 Oulu, Finland

Received 22 January 2001; accepted 9 March 2001

Abstract

Reductive elimination, the final step of the Monsanto and Cativa processes, has been studied using the density functional theory with the hybrid B3LYP exchange and correlation functional. To our knowledge, this is the first systematic computational study of the reductive elimination for which even the experimental studies are rare. We have studied different isomers of the anionic dicarbonyls $[Rh(CO)_2(COCH_3)I_3]^-$ (**1**) and $[Ir(CO)_2(COCH_3)I_3]^-$ (**2**). Several possible reaction routes for the elimination of CH_3COI from **1** and **2** have been explored. In addition, different isomers of the neutral tricarbonyl $[Ir(CO)_3(COCH_3)I_2]$ (**3**) and possible reaction paths connected to **3** have been studied. Our results show *mer*,*trans*-**1** to be the dominant intermediate in the rhodium system although its transformation to *fac*,*cis*-**1** and the elimination from this seems to be the most likely reaction pathway. In the anionic iridium system, the dominating intermediate is proposed to be *fac*,*cis*-**2**. In the neutral iridium system, *mer*,*cis*-**3** is proposed to be the dominant intermediate. While inspecting the iridium system as a whole, one could propose a transformation from anionic dicarbonyl to neutral tricarbonyl that would enhance the total rate of the reductive elimination. This observation is similar to that already verified in the 1,1-insertion in the Cativa process. In general, the geometrical arrangement of the different ligands has a large effect on the catalytic activity of the different possible intermediates of these processes.

Keywords: Rhodium; Iridium; Density functional theory; Catalysis; Elimination

1. Introduction

The catalytic carbonylation of methanol by the Monsanto or Cativa processes is an efficient method to manufacture acetic acid industrially. The main advantages of these procedures are low temperature and pressure needed. Several experimental and computational studies for the mechanism, kinetics and thermodynamics of these processes exist [1–9]. The active catalytic species in the Monsanto process is a diiododicarbonylrhodate anion $[Rh(CO)_2I_2]^-$. In the Cativa process the catalyst is an analogous iridium complex $[Ir(CO)_2I_2]^-$. A proposed catalytic cycle for the Monsanto process is illustrated in Fig. 1; the cycle for the Cativa process is basically very similar.

So far, we have studied the catalysts $[M(CO)_2I_2]^-$ (M = Rh and Ir) and their possible isomerizations from the *cis* to *trans* forms [8]. These results showed that previously unidentified *trans* forms of the active species are actually possible and reasonable isomerization paths exist. In addition, we have tested the *trans* forms of the active species in the first two reactions of the Monsanto and Cativa processes [9]. This work also included a systematic study of the possible isomers of the intermediates of the Monsanto and Cativa processes. In this paper, the finishing reactions of these catalytic cycles have been studied. We have calculated different structures of the octahedral intermediate complexes $[Rh(CO)_2(COCH_3)I_3]^-$ (**1**), $[Ir(CO)_2(COCH_3)I_3]^-$ (**2**) and $[Ir(CO)_3(COCH_3)I_2]$ (**3**). The reductive elimination has been studied using a variety of possible reaction routes. A reaction scheme for the reductive elimination is also shown in Fig. 1 [2,3]. Studies of the Monsanto and Cativa processes have so far been focused mainly on the first two reactions, the

* Corresponding author. Tel.: +358-8-5531640; fax: +358-85-531603.

E-mail addresses: tapani.kinnunen@oulu.fi (T. Kinnunen), kari.laasonen@oulu.fi (K. Laasonen).

0022-328X/01/$ - see front matter
PII: S0022-328X(01)00800-2

oxidative addition and 1,1-insertion. To our knowledge, this is the first systematic computational study of the reductive elimination. The experimental studies of the reaction mechanism and structures involved are few and the total picture of the Monsanto and Cativa processes could be improved by exploring the reductive elimination. The study of the reaction mechanism is important especially in the iridium system where the behavior of the structures involved in the catalytic cycle is more complex; the iridium cycle consists of both anionic and neutral pathways. Experimental studies are based mainly on the spectroscopic measurements that give information only on the dominant species present and species that could be very active in the actual reactions may not be observed. This gives the motivation to study a variety of different possible conformations and their reactivity.

2. Computational details

Density functional calculations have been based on the hybrid B3LYP [10,11] exchange and correlation (XC) functional and GAUSSIAN-98 [12] program packages. The basis set used here is denoted as SDD, which consists of a D95V for carbon, oxygen and hydrogen atoms. Stuttgart–Dresden effective core potentials (ECP) with scalar relativistic corrections have been used for rhodium, iridium and iodine. An extra fine integration grid has been employed. The methods that have been used here are the same as that in our previous studies [8,9]. These methods have worked well and therefore we are confident that the computational scheme is sufficient.

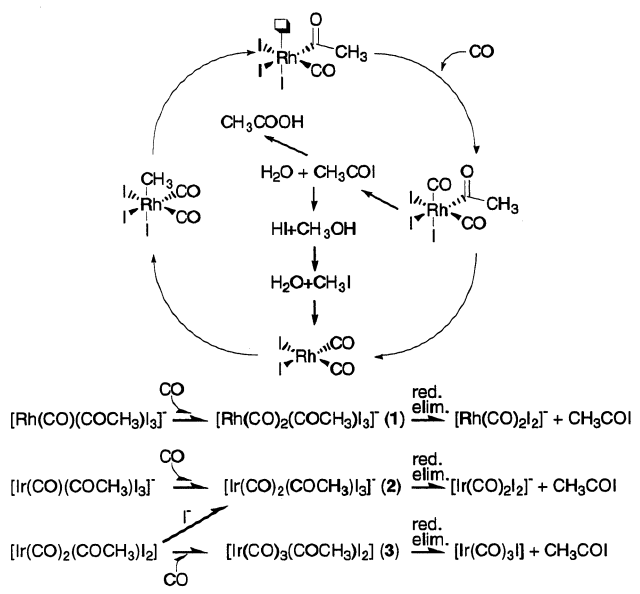

Fig. 1. A proposed mechanism for the Monsanto process and the reaction scheme for the reductive elimination in the Monsanto and Cativa processes.

The Berny optimization algorithm has been used to obtain the minimum energy and transition state structures. Rough structures of the transition states have been determined with potential energy surface (PES) scans. The PES has been scanned with a constrained optimization along a chosen internal coordinate.

Verification of the minimum energy and the transition state geometries has been done with frequency analyses. The transition states have one imaginary frequency. In the minimum energy structures all modes are real. An approximation for the free energies has also been acquired through the frequency analyses. The free energies reported here have been approximated at 298.15 K. All the results presented here have been acquired without any symmetry constraints in a gas phase. All the structures have been calculated as singlet states due to quite large HOMO–LUMO gaps.

The effect of solvation has been tested with the PCM [13] calculations using methanol as a solvent. These calculations show that the PCM changes the gas phase numbers slightly but the trends in the energy differences of the different isomers and the activation parameters are practically the same as in the gas phase results.

3. Results and discussion

3.1. The octahedral intermediate complexes $[M(CO)_2(COCH_3)I_3]^-$ (M = Rh and Ir)

Reactant complexes in the reductive elimination are anionic $[Rh(CO)_2(COCH_3)I_3]^-$ (**1**) and $[Ir(CO)_2(COCH_3)I_3]^-$ (**2**). As shown in the reaction scheme of Fig. 1, these are derived from five-coordinated acyl complexes $[M(CO)(COCH_3)I_3]^-$ (M = Rh and Ir) by carbon monoxide association [2,3]. If neutral tricarbonyl $[CH_3Ir(CO)_3I_2]$ is used in the 1,1-insertion [14], **2** is formed by iodide association [2,3] (see Fig. 1). In the latter case, carbon monoxide association can also take place (discussed later). Since the associating ligand attaches to a vacant site, both CO and iodide associations are expected to be very fast (discussed briefly later). Experiments indicate that the five-coordinated precursors of **1** and **2** are very fluxional [5,15], so any conformation of **1** and **2** is a possible intermediate after CO/I^- association.

Optimized geometries of *mer*,*trans*-, *mer*,*cis*- and *fac*,*cis*-isomers of **1** and **2** are presented in Fig. 2. Energy differences show the *mer*,*trans*-forms of **1** and **2** being most stable while the *mer*,*cis*-forms are less stable. The energy difference between *mer*,*trans*-**2** and *fac*,*cis*-**2** is very small, whereas the difference between *mer*,*trans*-**1** and *fac*,*cis*-**1** is larger. The results are shown in Table 1. The relative stabilities show a clear correlation to the structures (see Fig. 2). In the *fac*,*cis*-structures, the M–I (*trans* to the acyl group) bond is

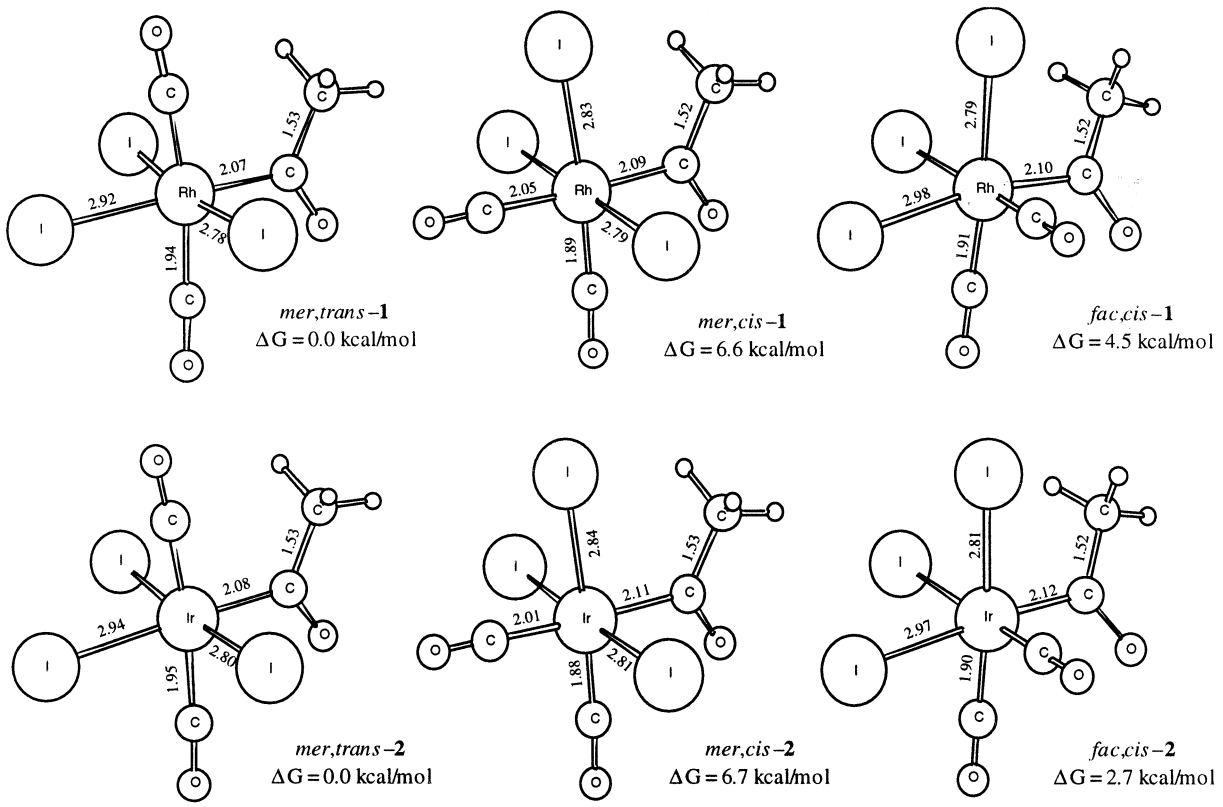

Fig. 2. The minimum energy structures of the different isomers of the anionic dicarbonyls **1** and **2**. The distances are given in Å. The relative free energies are calculated by comparing the *mer*,*trans*-isomers of **1** and **2**.

longer and therefore weaker than the corresponding bond in the *mer*,*trans*-structures. In the most unstable *mer*,*cis*-structures, the M–C (CO *trans* to the acyl group) bonds are weaker than M–C (CO *cis* to the acyl group). The presence of the acyl group *trans* to CO seems to have a destabilizing effect on the structure, indicating strong *trans* influence of the acyl group on CO. In **2** the structural deviations are smaller.

Experimental IR data are available for **1** and **2**; for **1**, NMR data also exist. In the rhodium system, the dominant species is proposed to be *mer*,*trans*-**1**. Both the IR and NMR data support this [5]. IR data show one strong and one very weak CO stretch; $^{13}C-^{13}C$ coupling constants from NMR are consistent with the *trans* carbonyls. The calculated CO-stretching modes in Table 2 show one strong and one weak CO stretch for *mer*,*trans*-**1**. For *mer*,*cis*- and *fac*,*cis*-**1**, the calculations show two CO modes of similar intensity. According to the calculated CO-stretching modes and the energy differences, our results also support *mer*,*trans*-**1** as the dominant species. For the iridium system, experimental IR data [2] show two strong CO-stretching modes indicating the *cis* arrangement of the carbonyls. The calculated CO-stretching modes of **2** have the same trends as those for **1** (see Table 2). CO modes of both *mer*,*cis*- and *fac*,*cis*-**2** are consistent with the experiments but the dominant species most probably has a *fac*,*cis*-conformation, which according to the calculations is clearly preferred. According to our calculations, *mer*,*trans*-isomer is the lowest energy form of **2**, so unlike in the rhodium system, the computational results differ from the experimental results. However, in the iridium system the energy difference between the *mer*,*trans*- and *fac*,*cis*-species is small and considering the general accuracy of the calculations, either *mer*,*trans*- or *fac*,*cis*-structure cannot be considered to be the dominant one. On the other hand, the experimental data do not rule out *mer*,*trans*-**2**. The calculated

Table 1
The relative stabilities between the different isomers of $[Rh(CO)_2(COCH_3)I_3]^-$ (**1**) and $[Ir(CO)_2(COCH_3)I_3]^-$ (**2**). The values are given in kcal mol^{-1}, total energies including the zero-point correction. Energy differences are relative to *mer*,*trans*-**1** and *mer*,*trans*-**2**

Species	ΔE	ΔG
mer,*trans*-**1**	0.0	0.0
mer,*cis*-**1** conf. 1	6.8	6.6
mer,*cis*-**1** conf. 2	10.9	10.4
fac,*cis*-**1**	5.0	4.5
mer,*trans*-**2**	0.0	0.0
mer,*cis*-**2** conf. 1	6.8	6.7
mer,*cis*-**2** conf. 2	10.7	10.2
fac,*cis*-**2**	2.8	2.7
fac,*cis*-**2** conf. 2	8.5	7.8

Table 2
The calculated free CO-stretching modes of the different isomers of **1** and **2**. Wave numbers are given in cm^{-1}. The intensities of the modes are given in parentheses

CO modes	ν_1	ν_2
mer,*trans*-**1**	1991.9 (1005)	2054.0 (62)
mer,*cis*-**1** conf. 1	1987.5 (406)	2021.4 (559)
fac,*cis*-**1**	1994.5 (414)	2028.8 (576)
mer,*trans*-**2**	1981.6 (1164)	2061.5 (44)
mer,*cis*-**2** conf. 1	1977.3 (520)	2023.8 (587)
fac,*cis*-**2**	1988.2 (520)	2034.8 (605)

higher wave number symmetric stretch for *mer*,*trans*-**2** has even lower intensity than that calculated for *mer*,*trans*-**1** (see Table 2). Very low intensity symmetric stretch would be difficult to observe and lower wave number antisymmetric mode would overlap with the antisymmetric mode from the *cis* carbonyls.

In **1** and **2**, the acyl group can obtain different orientations by a rotation with respect to the M–C (acyl group) bond. The acyl group rotation is hindered sterically by the large iodides [5] and the rotation barrier is proposed to be relatively high. We have scanned the PES according to the acyl group rotation in the different isomers of **1** and **2**, and for these scans we evaluate the total energy barriers of 10 kcal mol^{-1} in *mer*,*trans*-**1** and 9 kcal mol^{-1} in *mer*,*trans*-**2**. In the *mer*,*cis*-isomers of **1** and **2**, the rotation barriers are 5 kcal mol^{-1} and in the *fac*,*cis*-isomers of **1** and **2**, the barriers are 6 kcal mol^{-1}.

For *mer*,*cis*-**1**, *mer*,*cis*-**2** and *fac*,*cis*-**2**, we have located a higher energy conformation where the acyl group has inverted. The energy differences between these and other isomers of **1** and **2** are shown in Table 1. For *mer*,*trans*-**1**, *mer*,*trans*-**2** and *fac*,*cis*-**1**, similar stationary points have not been found.

According to the computed results, the rotation of the acyl group is expected to take place in the different isomers of **1** and **2**, because the rotation barriers are not very high. For *mer*,*cis*-**1** and *mer*,*cis*-**2** the rotation of the acyl group may have significance since their PES have clearly higher energy minima that could participate to the actual elimination. The PES of *fac*,*cis*-**2**, with respect to the rotation, has only a very shallow higher energy minimum.

3.2. The reductive elimination from $[M(CO)_2(COCH_3)I_3]^-$ (M = Rh and Ir)

In the Monsanto and Cativa processes the reductive elimination concludes the catalysis cycles. In general, the elimination is proposed to proceed through a three-centered transition state resulting in the regeneration of the catalyst $[M(CO)_2I_2]^-$ (M = Rh and Ir) and formation of acetyl iodide. The metal center reduces from oxidation state III to I.

We have studied the elimination from the different isomers of **1** and **2**. In *mer*,*cis*-**1** and *mer*,*cis*-**2**, due to the positions of the iodides, two pathways for elimination are available (see Fig. 2). Both these pathways have been studied. The two pathways for the elimination available from the higher energy conformations of *mer*,*cis*-**1** and *mer*,*cis*-**2** have also been studied.

The calculated transition states are presented in Fig. 3. The second possible pathway for the eliminations from both the lower and higher energy conformations of *mer*,*cis*-**1** and *mer*,*cis*-**2** lead to the same transition state. In all other reaction paths studied, the transition states are distinct. The structures of the transition states depend on whether carbon monoxide or iodide is in *trans* position to the eliminated acyl group. If iodide is in *trans* position to the acyl group, the transition state has a quite long M–I (eliminating) distance, which is the case of eliminations from the *mer*,*trans*- and *fac*,*cis*-structures. In the *mer*,*cis*-structures, CO is in *trans* position to the acyl group and the transition states are quite 'early' with respect to the eliminated acetyl iodide part. The activation parameters for the eliminations studied are presented in Table 3. The geometrical arrangement of the ligands has some effect on the activation barriers. In the *fac*,*cis*-structures, carbon monoxide is in *trans* position to the eliminated iodide and the barriers are lower compared to the other geometries. In the *mer*,*trans*-structures, iodides are in *trans* positions to both the eliminated ligands and the barriers are higher than in the *fac*,*cis*-systems. The elimination from the *mer*,*cis*-structures can proceed through two different reaction paths. In both these paths, carbon monoxides are in *trans* position to the eliminated acyl group. In the first path, iodide is *trans* to the eliminated iodide and the barrier is quite high. In the second path, CO is *trans* to the eliminated iodide and the barrier is lower than in the first path. Our results show that the reductive elimination is also possible in the higher energy conformations of *mer*,*cis*-**1** and *mer*,*cis*-**2**. The calculated activation entropies for the eliminations studied are small. The approximated experimental activation enthalpy for the reductive elimination in the rhodium system is 87 kJ mol^{-1} (ca. 21 kcal mol^{-1}) with the activation entropy of 43 J K^{-1} mol^{-1} (ca. 0.01 kcal K^{-1} mol^{-1}) [4], so our computational results are similar. The activation barriers of the elimination in the iridium system are higher than the rhodium system. In general, the activation barriers of the elimination studied are quite high. This is in agreement with the experimental data that, in the rhodium system, show the reductive elimination becomes the rate-determining step if the reaction temperature is lowered [4]. The oxidative addition is the rate-determining step of the Monsanto process in 'normal' reaction conditions.

Even though there are several possible reaction pathways for the reductive elimination from the different

isomers of **1** and **2**, there are only two products. The reductive eliminations from *mer*,*trans*-**1** and *mer*,*trans*-**2** result in *trans*-$[M(CO)_2I_2]^-$ (M = Rh and Ir) and acetyl iodide. This is also the product of the second reaction path for the elimination from both lower and higher energy conformations of *mer*,*cis*-**1** and *mer*,*cis*-**2**. In both the rhodium and iridium systems, the product complexes are 7.2 kcal mol^{-1} lower in energy than the

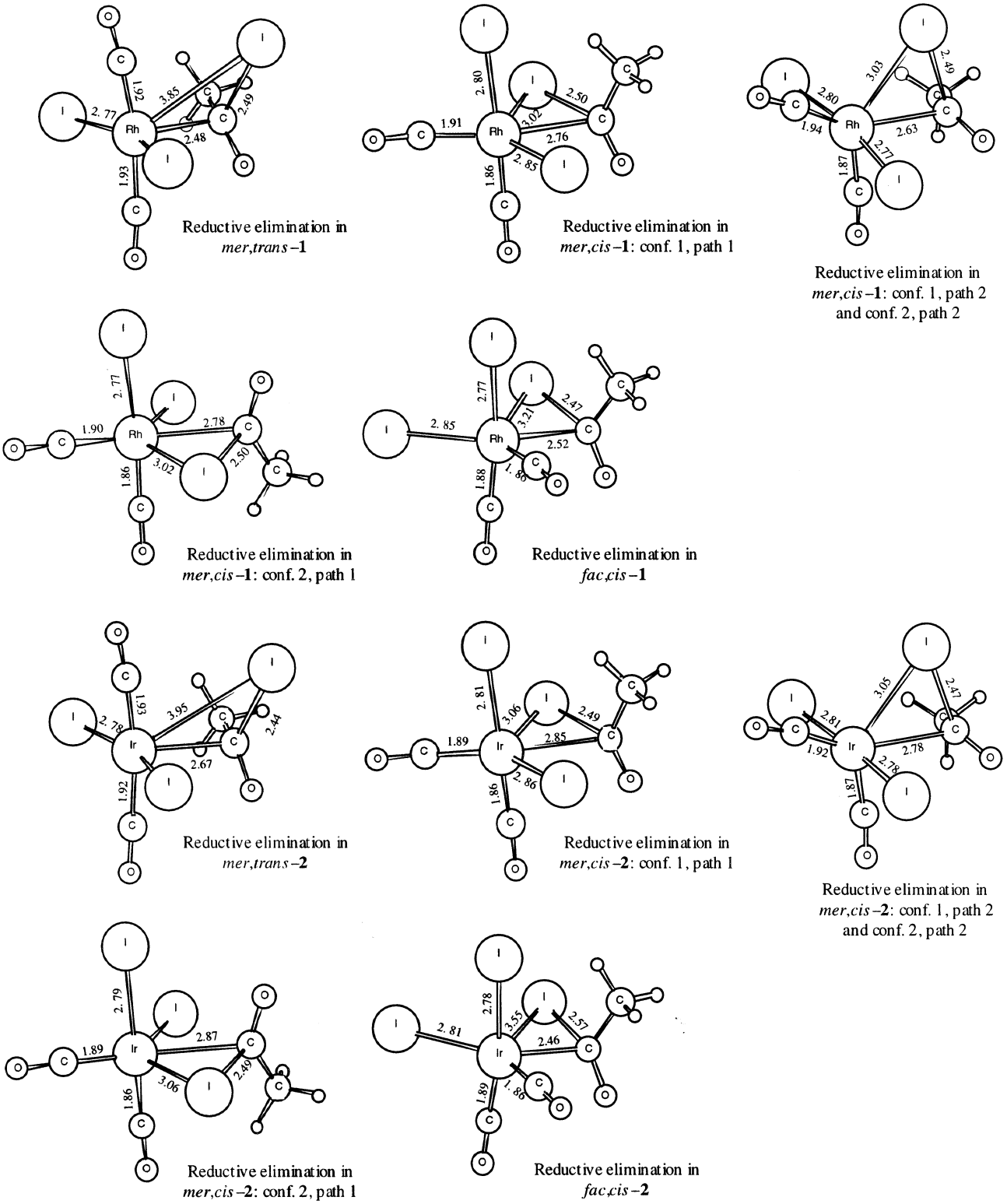

Fig. 3. The transition states of the reductive eliminations from the different isomers of **1** and **2**. Distances are given in Å.

Table 3
Activation parameters and reaction energies of the reductive elimination studied in structures **1** and **2**. The values are given in kcal mol^{-1} and total energy values include zero-point corrections

Elimination form	ΔE [a]	ΔG [a]	ΔE [b]	ΔG [b]
mer,*trans*-**1**	25.8	25.1	11.9	5.0
mer,*cis*-**1** conf. 1, path 1	26.4	26.4	−1.5	−6.7
mer,*cis*-**1** conf. 1, path 2	23.8	23.9	5.1	−1.6
mer,*cis*-**1** conf. 2, path 1	25.5	25.7	−5.5	−10.6
mer,*cis*-**1** conf. 2, path 2	19.8	20.1	1.0	−5.4
fac,*cis*−**1**	22.1	22.6	0.4	−4.6
mer,*trans*-**2**	35.9	35.0	22.9	16.4
mer,*cis*-**2** conf. 1, path 1	35.4	35.5	4.6	−0.7
mer,*cis*-**2** conf. 1, path 2	32.6	32.8	16.1	9.7
mer,*cis*-**2** conf. 2, path 1	34.5	35.0	0.6	−4.2
mer,*cis*-**2** conf. 2, path 2	28.7	29.3	12.1	6.2
fac,*cis*-**2**	29.0	28.6	8.5	3.3

[a] Denotes activation parameters.
[b] Denotes reaction energy.

sum of the total energies of *trans*-catalyst and acetyl iodide calculated at infinite separation. The *fac*,*cis*-systems and first reaction paths in both lower and higher energy conformations of the *mer*,*cis*-structures result in *cis*-$[M(CO)_2I_2]^-$ (M = Rh and Ir) and acetyl iodide. In the rhodium system, the product complex is 8.1 kcal mol^{-1} more stable than the *cis* form of the catalyst and acetyl iodide at infinite separation. For the iridium, the corresponding energy is 7.9 kcal mol^{-1}. The structures of the product complexes are presented in Fig. 4 and the computed reaction energies of the reductive elimination studied are given in Table 3. In all the elimination studies, the quite large positive reaction entropies are understandable because one molecule splits into two. The difference in the reaction energies is derived from the energy difference between the isomers of **1** and **2** and, on the other hand, there are two dissimilar product possibilities, *cis*- or *trans*-catalyst and CH_3COI. In our previous study [8], we found the *cis*–*trans* free energy difference of 4.9 kcal mol^{-1} in the rhodium system and 10.4 kcal mol^{-1} in the iridium system, *cis* isomers in both systems being more stable.

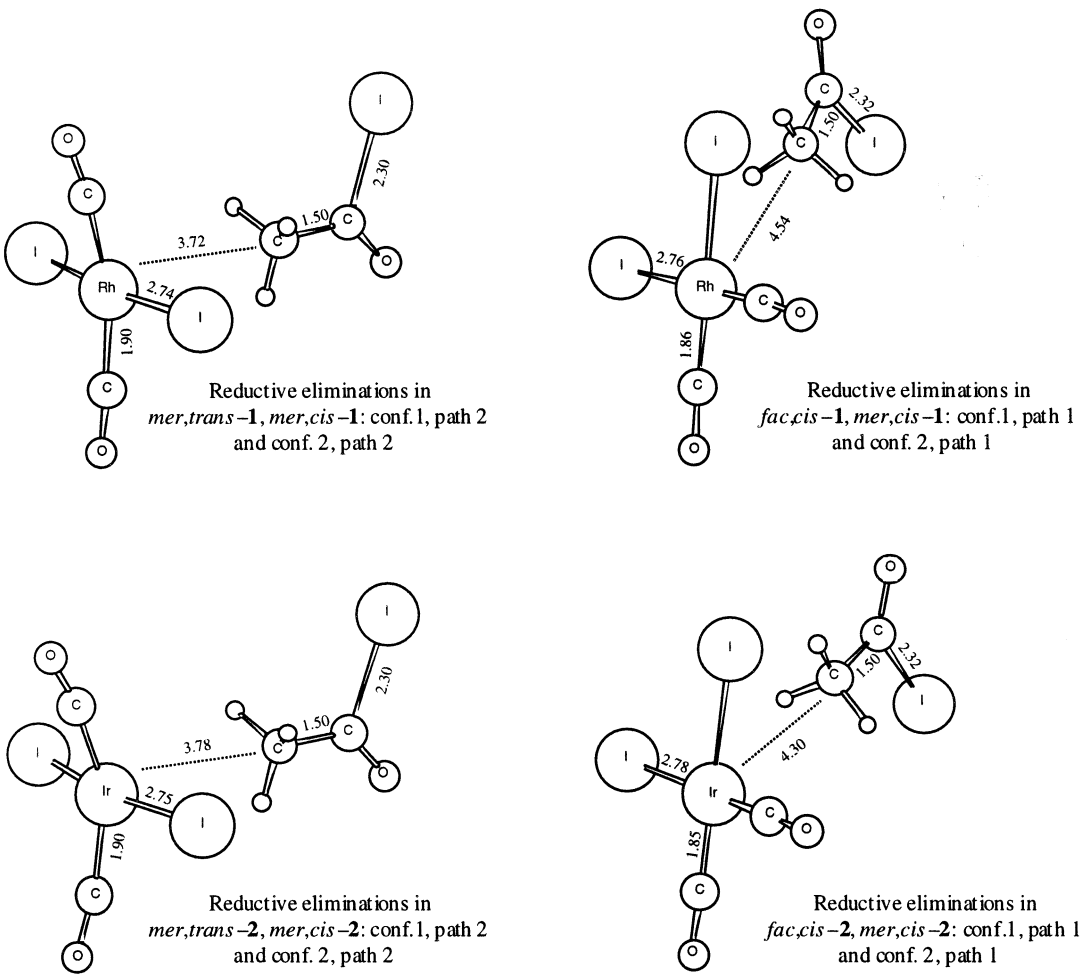

Fig. 4. The product complexes of the different reductive eliminations studied in the different isomers of **1** and **2**. The distances are given in Å.

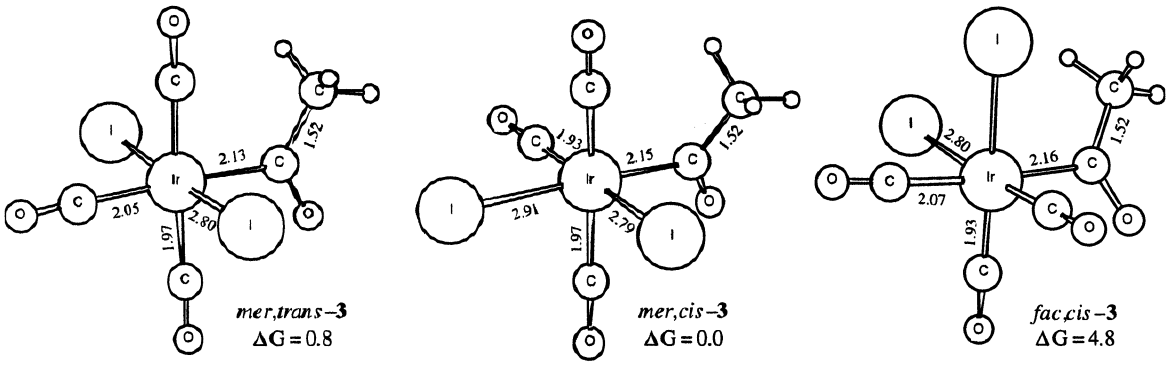

Fig. 5. The minimum energy structures of the different isomers of the neutral tricarbonyl **3**. The distances are given in Å. The relative free energies are calculated by comparing *mer*,*cis*-**3**.

3.3. The dissociation of carbon monoxide or iodide from $[M(CO)_2(COCH_3)I_3]^-$ (M = Rh and Ir)

The dominant intermediate structure of **1** is proposed to be *mer*,*trans*-**1**. The experimentalists have proposed that this dominating species undergoes a transformation to *fac*,*cis*-isomer [5]. This suggestion is based on the assumption that the reductive elimination from *mer*,*trans*-**1** produces the *trans* form of the active catalyst. The *trans* form is so far unobserved by the experimental studies and elimination from *mer*,*trans*-**1** is considered impossible [5]. However, we have shown previously that the *trans* forms of the active species, both in the rhodium and iridium systems, are possible [8] and as discussed in Section 3.2, the elimination from *mer*,*trans*-**1** can take place.

We have studied carbon monoxide and iodide dissociations from the dominant intermediate *mer*,*trans*-**1** to make comparisons to the model proposed by the experimentalists. The calculated free energy barrier of CO dissociation is 24.6 kcal mol^{-1}, which is slightly lower than the barrier of the reductive elimination from *mer*,*trans*-**1** (see Table 3). We have studied the iodide dissociation with the PES scans that shows the iodide dissociation to have a lower barrier than the reductive elimination from *mer*,*trans*-**1**. This supports the assumption that *mer*,*trans*-**1** could be transformed to other isomers. For the iridium system, the proposed dominant intermediate is *fac*,*cis*-**2** and we have studied the CO or iodide dissociation from it. Also, the iodide dissociation is possible and the *fac*,*cis*-**2** could be transformed to other isomers. The CO dissociation in the iridium system seems unlikely, its free energy barrier is 33.8 kcal mol^{-1}.

As mentioned previously, the CO association forms **1** in the rhodium system (see Fig. 1). With the PES obtained from the CO-dissociation study, we evaluate the total energy barrier of about 10 kcal mol^{-1} for the CO association in the rhodium system. This is not the barrier of the CO association to the vacant site of the five-coordinated product of the dissociation but we can assume that the barrier of the CO association to the vacant site is even smaller, and therefore the CO association is easy. Depending on the history of the iridium complex the CO or iodide association forms **2**. Here, the evaluated total energy barrier of the CO association is slightly higher than the rhodium system. Again, this is not the barrier of the association to the vacant site but it shows that the CO association in the iridium system is also easy. According to the PES scan, the iodide association seems to be very easy.

3.4. The octahedral intermediate complex $[Ir(CO)_3(COCH_3)I_2]$

As mentioned earlier, if the neutral tricarbonyl complex participates to the 1,1-insertion, the carbon monoxide addition leads to $[Ir(CO)_3(COCH_3)I_2]$ (**3**) (see Fig. 1). This complex takes part in the neutral part of the catalysis cycle in the iridium system.

We have studied *mer*,*trans*-, *mer*,*cis*- and *fac*,*cis* isomers of **3** and the optimized structures are shown in Fig. 5. Calculated energy differences show *mer*,*cis*-**3** being the most stable but *mer*,*trans*-**3** is only marginally less stable. The most unstable isomer is *fac*,*cis*-**3**. The energy differences are shown in Table 4. Also, the energy differences correlate to the structures (see Fig. 5). The M–C (*trans* to the acyl group) bond in *fac*,*cis*-**3** is weaker than it is in *mer*,*trans*-**3**. Again, the structures

Table 4
The relative stabilities between different isomers of $[Ir(CO)_3(COCH_3)I_2]$ (**3**). The values are given in kcal mol^{-1}, total energies including the zero-point correction. Energy differences are given relative to *mer*,*cis*-**3**

Species	ΔE	ΔG
mer,*trans*-**3**	1.1	0.8
mer,*cis*-**3**	0.0	0.0
fac,*cis*-**3**	4.6	4.8

Table 5
The calculated free CO-stretching modes of the different isomers of **3**. Wave numbers are given in cm^{-1}. The intensities of the modes are given in parentheses

CO mode	ν_1	ν_2	ν_3
mer,*trans*-**3**	2033.1 (544)	2044.3 (805)	2114.1 (55)
mer,*cis*-**3**	2035.1 (584)	2047.6 (839)	2108.4 (99)
fac,*cis*-**3**	2030.4 (480)	2039.3 (413)	2082.2 (523)

Table 6
Activation parameters and reaction energies of the reductive elimination studied in **3**. The values are given in kcal mol^{-1} and total energy values include zero-point corrections

Elimination from	ΔE [a]	ΔG [a]	ΔE [b]	ΔG [b]
mer,*trans*-**3**	27.9	28.1	5.7	0.7
mer,*cis*-**3**	24.5	24.5	6.8	1.5
fac,*cis*-**3**	19.5	19.9	2.1	−3.3

[a] Denotes activation parameters.
[b] Denotes reaction energy.

with CO instead of iodide *trans* to the acyl group are destabilized and now *mer*,*cis*-**3** with iodide *trans* to the acyl group is the most stable (compare the energy differences and structures in case of **1** and **2**, Fig. 2 and Table 1).

There are also some IR data for the neutral part of the iridium system. Here, the experiments show one strong and one weak CO-stretching mode [2]. This is consistent with both *mer*,*trans*-**3** and *mer*,*cis*-**3** for which our calculations show three CO-stretching modes. The data are presented in Table 5. The computed lower wave number CO modes of *mer*,*trans*-**3** and *mer*,*cis*-**3** are very close and in the experimental spectrum only two peaks are observed. The experimentally observed weak higher wave number peak is consistent with both *mer*,*trans*-**3** and *mer*,*cis*-**3** but we propose *mer*,*cis*-**3** as the dominant intermediate, since its higher wave number CO mode is clearly more intense than the corresponding CO mode of *mer*,*trans*-**3**. Also, *mer*,*cis*-**3** is the most stable isomer of **3** although the energy difference to *mer*,*trans*-**3** is only marginal. The higher wave number CO-stretching mode of *fac*,*cis*-**3** has strong intensity and it is separated clearly from the peaks of the other isomers but *fac*,*cis*-**3** is not observed.

Like in the case of the dicarbonyls **1** and **2**, we have studied whether different orientations of the acyl group exist. Using the PES scans we have evaluated the rotational energy barrier of 4 kcal mol^{-1} for the *mer*,*trans*-**3** and 5 kcal mol^{-1} for *fac*,*cis*-**3** and *mer*,*cis*-**3**. This shows that the rotation is possible but its significance to the elimination is limited because we have not found other conformations of the different isomers of **3**.

3.5. The reductive elimination from $[Ir(CO)_3(COCH_3)I_2]$

In the neutral part of the iridium system, the reductive elimination proceeds similarly as in the anionic part but the reaction produces four-coordinated neutral species $[Ir(CO)_3I]$ and acetyl iodide. Also, the metal center reduces from oxidation state III to I.

We have studied the reductive elimination from *mer*,*trans*-**3**, *mer*,*cis*-**3** and *fac*,*cis*-**3**. The calculated transition states are presented in Fig. 6 and the activation parameters in Table 6. Here the transition states are all similar with respect to the Ir–C (acyl group), Ir–I (eliminating) and C (acyl group)–I (eliminating) bond lengths, and the transition states are all quite 'early'. However, the activation barriers are different. The reductive elimination from *fac*,*cis*-**3** has clearly the lowest free energy of activation, elimination from *mer*,*trans*-**3** has the highest free energy barrier and the free energy barrier of the elimination from *mer*,*cis*-**3** is in middle, when compared with the previous case (see Table 6). The computed activation entropies are small. Also, the geometrical arrangement of the ligands correlates with

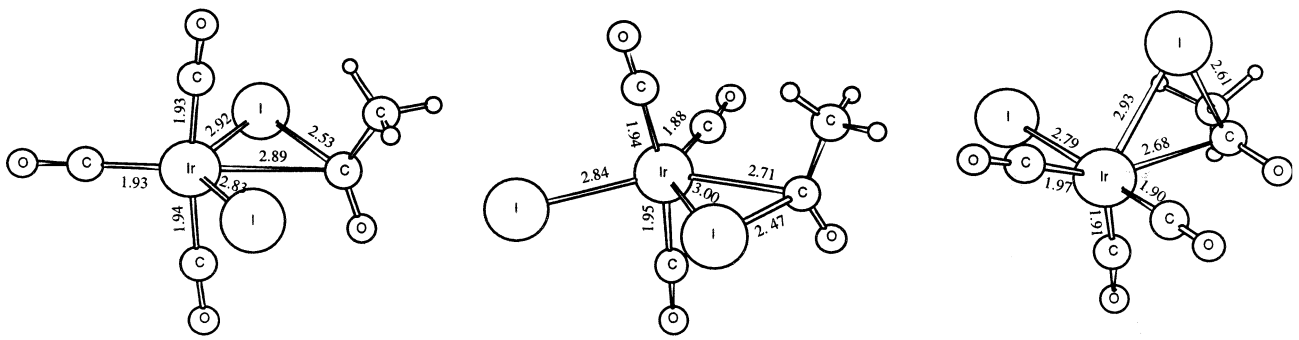

Fig. 6. The transition states of the reductive eliminations from the different isomers of **3**. Distances are given in Å.

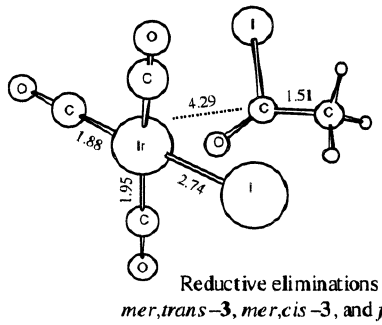

Fig. 7. The product complex of the different reductive eliminations studied in the different isomers **3**. The distances are given in Å.

the activation barriers. In *fac*,*cis*-**3**, carbon monoxides are in *trans* position to both acyl group and the eliminated iodide. In *mer*,*trans*-**3**, CO is *trans* to the acyl group and in *mer*,*cis*-**3**, CO is *trans* to the eliminated iodide (see Figs. 5 and 6). Also, the *trans* effect of the CO to the eliminated ligands has some influence on the elimination barriers. Thus it can be concluded that the CO in *trans* position to the eliminated iodide has more effect on the elimination barrier than the CO in *trans* position to the acyl group has (see Figs. 2 and 5, Tables 3 and 6).

The eliminations from all the isomers of the tricarbonyl **3** lead to neutral $[Ir(CO)_3I]$ and acetyl iodide. The product complex is presented in Fig. 7 and the computed result shows it being 3.0 kcal mol^{-1} lower in the total energy than the truly separated molecules. The reaction energies of the different eliminations are shown in Table 6. Like in the case of the dicarbonyls, the reaction entropies are positive. The difference in the reaction energies is derived from the energy differences of the different isomers of **3**.

3.6. The dissociation of carbon monoxide or iodide from $[Ir(CO)_3(COCH_3)I_2]$

As seen in Section 3.5, there are differences in the activation barriers of the eliminations in different forms of the tricarbonyl **3**. Thus it is important to know if a transformation from the dominant intermediate structure to some other structure could take place.

Here we have studied the dissociation of CO or iodide from *mer*,*cis*-**3** that is supposed to be the dominant isomer of **3**. For the CO dissociation, the lowest free energy barrier that we find is 25.5 kcal mol^{-1}, so the reductive elimination from *mer*,*cis*-**3** is easier than the CO dissociation (see Table 6). The iodide dissociation has been studied with the PES scans and it is unlikely because the barrier for the elimination from *mer*,*cis*-**3** is lower than the barrier of the dissociation. The reductive elimination from *mer*,*cis*-**3** is easier than the carbon monoxide or iodide dissociation and the transformation of *mer*,*cis*-**3** to some other isomer is insignificant for the reductive elimination.

As in the dicarbonyl system, with the PES obtained from the CO-dissociation studies, some conclusions of the CO association can be made. For the CO association, the total energy barrier is slightly over 10 kcal mol^{-1}. The association of the CO is quite easy even though the barrier described here is not the barrier to the vacant site of the five-coordinated product of the CO dissociation.

4. Conclusions

We have studied reductive elimination, the concluding reaction of the Monsanto and Cativa processes. The

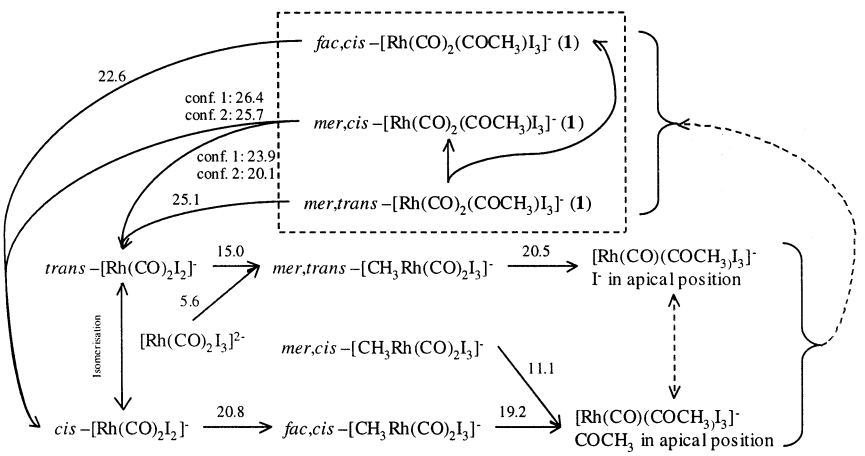

Fig. 8. The overall scheme of the Monsanto process showing the possible structures and reaction routes studied in the rhodium system. The structures in the dashed box feature the current study. Other structures are from our previous studies [8,9]. Solid arrow indicates that the corresponding process is expected to occur. Dashed arrow indicates that corresponding process is expected to take place but we have no specific data from it. Missing arrow between two structures indicates that there is no knowledge if or how the transformation takes place. Numbers shown are the calculated free energy barriers in kcal mol^{-1} for the corresponding processes. The numbers shown for the reactions other than the eliminations are from Ref. [9].

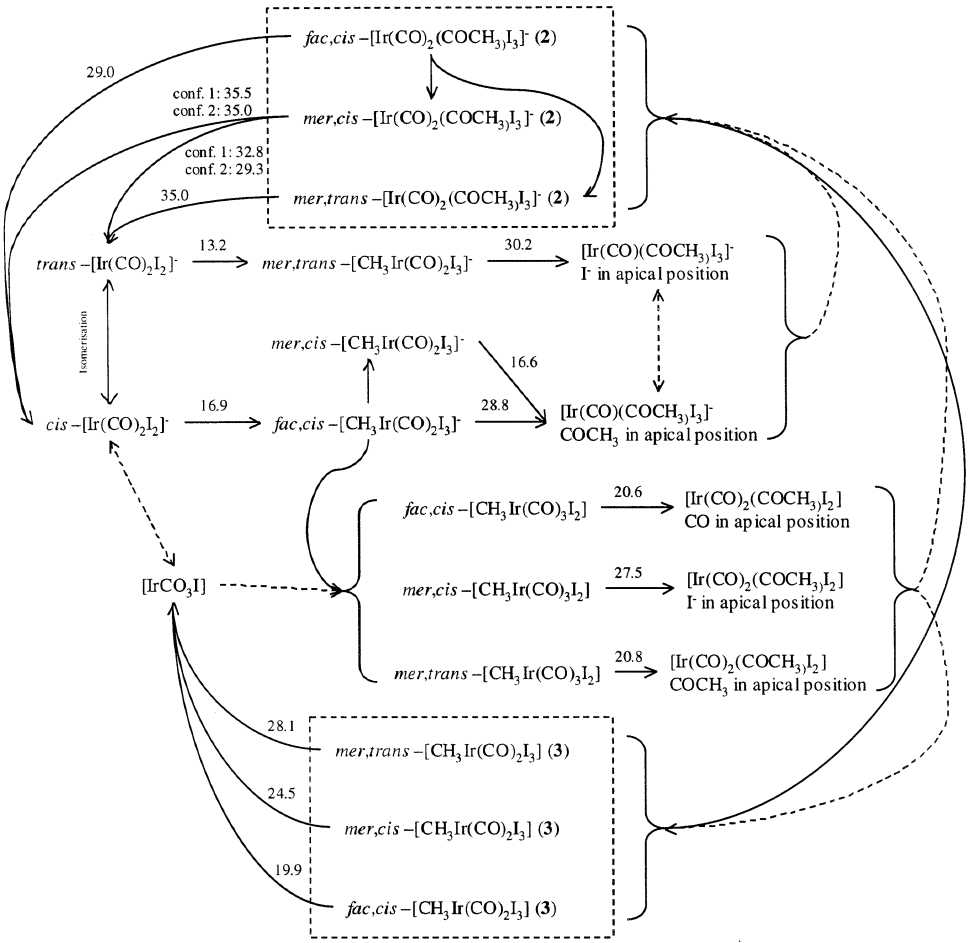

Fig. 9. The overall scheme of the Cativa process showing the possible structures and reaction routes studied in the iridium system. The structures in the dashed box feature the current study. Other structures are from our previous studies [8,9]. Solid arrow indicates that the corresponding process is expected to occur. Dashed arrow indicates that corresponding process is expected to take place but we have no specific data from it. Missing arrow between two structures indicates that there is no knowledge if or how the transformation takes place. Numbers shown are the calculated free energy barriers in kcal mol^{-1} for the corresponding processes. The numbers shown for the reactions other than the eliminations are from Ref. [9].

different isomers and conformations of the intermediate structures $[Rh(CO)_2(COCH_3)I_3]^-$ (**1**), $[Ir(CO)_2(COCH_3)I_3]^-$ (**2**) and $[Ir(CO)_3(COCH_3)I_2]$ (**3**) have been investigated. A systematic study of the reductive elimination from the different possible structures has been conducted. The intermediate structures and reaction possibilities involved, including the calculated free energies of activation are presented schematically in Fig. 8 for the rhodium system and in Fig. 9 for the iridium system. We would like to illustrate the complete process of the studied catalysis, so Figs. 8 and 9 include the intermediates and reaction paths explored in our previous studies [8,9].

For the reductive elimination part we conclude the following. In the rhodium system, the proposed dominant intermediate structure is *mer,trans*-**1**. The experimentalists have proposed that this isomer undergoes a transformation and the actual elimination proceeds via *fac,cis*-**1**. Our results show that the elimination from *mer,trans*-**1** is possible because the activation barrier is not very high but the transformation to some other isomer of **1** is more likely, since the barrier of the elimination from *mer,trans*-**1** is higher than the barrier of the transformation. The two lowest barriers calculated for the reductive elimination are in the second possible reaction pathway in higher energy conformation of *mer,cis*-**1** and in the *fac,cis*-**1**. From these, the elimination from *fac,cis*-**1** is more likely, since the free energy difference between *fac,cis*-**1** and the higher energy conformation of *mer,cis*-**1** is 5.9 kcal mol^{-1}. For the rhodium system, our results support the proposal of the experimentalists although our reasoning is different. The reason for the transformation from *mer,trans*-**1** to *fac,cis*-**1** is the lower elimination barrier in *fac,cis*-**1**, not the assumption that *trans*-$[Rh(CO)_2I_2]^-$ is non-existent.

In the anionic part of the iridium system, the proposed dominant intermediate is *fac,cis*-**2**. The calculated activation barriers of the different eliminations

studied here show that the most feasible reaction path is the elimination from *fac*,*cis*-**2**. Even the transformation of *fac*,*cis*-**2** to some other isomer is possible via iodide dissociation, the transformation is insignificant.

The computed results for the neutral part of the iridium system propose *mer*,*cis*-**3** as a dominating intermediate. The calculated activation barriers show that the easiest reaction path could be the reductive elimination from *fac*,*cis*-**3**. However, our results propose that the elimination from *mer*,*cis*-**3** is easier than its transformation to *fac*,*cis*-**3**, so the most likely reaction path is the reductive elimination from *mer*,*cis*-**3**.

In the entire iridium system, it seems that the reductive elimination in the neutral tricarbonyl system is easier than the elimination in the anionic dicarbonyl system. This is also the case in the crucial 1,1-insertion of the Cativa process [2,4,14]. Based on the previous results, we propose a similar reaction path for the reductive elimination that is verified for the 1,1-insertion; the dicarbonyl **2** could be transformed to the tricarbonyl **3** which would enhance the total rate of the reductive elimination. Of course, this would depend on the iodide concentration of the system. As in the case of the insertion, the neutral tricarbonyl part of the system is preferred in the low iodide concentration.

In general, as observed in our previous studies [9], in the reductive elimination the geometrical arrangement of the attached ligand has a large effect to the catalytic activity of the different structures.

Acknowledgements

The Graduate School of Computational Chemistry and Molecular Spectroscopy has provided the financial support for this work. The authors would like to thank The Finnish Center for Scientific Computing (CSC) for the computational resources.

References

[1] D. Forster, J. Am. Chem. Soc. 98 (1976) 846.
[2] D. Forster, J. Chem. Soc. Dalton Trans. (1979) 1639.
[3] T.W. Dekleva, D. Forster, Adv. Catal. 34 (1986) 81.
[4] P.M. Maitlis, A. Haynes, G.J. Sunley, M.J. Howard, J. Chem. Soc. Dalton Trans.(1996) 2187.
[5] H. Adams, N.A. Bailey, B.E. Mann, C.P. Manuel, C.M. Spencer, A.G. Kent, J. Chem. Soc. Dalton Trans. (1988) 489.
[6] T.R. Griffin, D.B. Cook, A. Haynes, J.M. Pearson, D. Monti, G.E. Morris, J. Am. Chem. Soc. 118 (1996) 3029.
[7] M. Cheong, R. Schmid, T. Ziegler, Organometallics 19 (2000) 1973.
[8] T. Kinnunen, K. Laasonen, J. Mol. Struct. (Theochem) 540 (2001) 91.
[9] T. Kinnunen, K. Laasonen, J. Mol. Struct. (Theochem) 542 (2001) 273.
[10] A.D. Becke, J. Chem. Phys. 98 (1993) 564.
[11] C. Lee, W. Yang, R.G. Parr, Phys. Rev. B 37 (1988) 785.
[12] M.J. Frisch, G.W. Trucks, H.B. Schlegel, G.E. Scuseria, M.A. Robb, J.R. Cheeseman, V.G. Zakrzewski, J.A. Montgomery, R.E. Stratmann, J.C. Burant, S. Dapprich, J.M. Millam, A.D. Daniels, K.N. Kudin, M.C. Strain, O. Farkas, J. Tomasi, V. Barone, M. Cossi, R. Cammi, B. Mennucci, C. Pomelli, C. Adamo, S. Clifford, J. Ochterski, G.A. Petersson, P.Y. Ayala, Q. Cui, K. Morokuma, D.K. Malick, A.D. Rabuck, K. Raghavachari, J.B. Foresman, J. Cioslowski, J.V. Ortiz, B.B. Stefanov, G. Liu, A. Liashenko, P. Piskorz, I. Komaromi, R. Gomperts, R.L. Martin, D.J. Fox,, T. Keith, M.A. Al Laham, C.Y. Peng, A. Nanayakkara, C. Gonzalez, M. Challacombe, P.M.W. Gill, B.G. Johnson, W. Chen, M.W. Wong, J.L. Andres, M. Head-Gordon, E.S. Replogle, J.A. Pople, GAUSSIAN-98 (Revision A.3), Gaussian Inc., Pittsburgh, PA, 1998.
[13] C.J. Cramer, D.G. Truhlar, Chem. Rev. 99 (1999) 2161.
[14] T. Ghaffar, H. Adams, P.M. Maitlis, G.J. Sunley, M.J. Baker, A. Haynes, Chem. Commun. (1998) 1023.
[15] A. Haynes, B.E. Mann, G.E. Morris, P.M. Maitlis, J. Am. Chem. Soc. 115 (1993) 4093.